Digital spatially incoherent Fresnel holography

Joseph Rosen*

Department of Biology, Integrated Imaging Center, Johns Hopkins University, Montgomery County Campus, Suite 240, 9605 Medical Center Drive, Rockville, Maryland 20850, USA

Gary Brooker

Department of Biology, Integrated Imaging Center, Johns Hopkins University, Montgomery County Campus, Suite 240, 9605 Medical Center Drive, Rockville, Maryland 20850, USA

Received November 17, 2006; revised December 19, 2006; accepted January 13, 2007; posted January 18, 2007 (Doc. ID 77217); published March 19, 2007

We present a new method for recording digital holograms under incoherent illumination. Light is reflected from a 3D object, propagates through a diffractive optical element (DOE), and is recorded by a digital camera. Three holograms are recorded sequentially, each for a different phase factor of the DOE. The three holograms are superposed in the computer, such that the result is a complex-valued Fresnel hologram. When this hologram is reconstructed in the computer, the 3D properties of the object are revealed. © 2007 Optical Society of America

OCIS codes: 090.0090, 090.1970, 070.4550, 110.6880, 100.3010, 050.1950.

Holograms recorded by incoherent light open many new applications such as outdoor and astronomical holography[1] and fluorescence holographic microscopy.[2] The oldest methods of recording incoherent holograms have made use of the property that every incoherent object is composed of many source points, each of which is self-spatial coherent and therefore can create an interference pattern with light coming from the point's mirrored image. Under this general principle, there are various types of holograms,[1,3–9] including Fourier[1,4] and Fresnel holograms.[5,6] The process of beam interfering demands high levels of light intensity, extreme stability of the optical setup, and relatively narrow bandwidth light source. These limitations have prevented holograms from becoming widely used for many practical applications.

More recently, two groups of researchers have proposed computing holograms of 3D incoherently illuminated objects from a set of images taken from different points of view.[10,11] This method, although it shows promising prospects, is relatively slow since it is based on capturing tens of scene images from different view angles.

Another method is called scanning holography,[2,12] in which a pattern of Fresnel zone plates (FZPs) scans the object such that at each and every scanning position, the light intensity is integrated by a point detector. The overall process yields a Fresnel hologram obtained as a correlation between the object and FZP patterns. However, the scanning process is relatively slow and is done by mechanical movements. A similar correlation is actually also done in this Letter; however, unlike the case of scanning holography, we propose here a correlation without movement.

Mertz and Young[13] already proposed holographic photography based on correlation without movement between objects and FZPs. However, their process relies on geometrical optics, which cannot yield good imaging results in the optical regime. On the contrary, our suggested correlator for implementing the holographic recording is valid in the optical regime, since its operation principle is based on the diffraction theory.[14]

Presented here is a new method of recording digital Fresnel holograms under incoherent illumination. We coin our new technique Fresnel incoherent correlation holography (FINCH). In our system, the reflected white light from a 3D object propagates through a diffractive optical element (DOE) and is recorded by a digital camera. Three holograms are recorded sequentially, each with a different phase factor of the DOE. The three holograms are superposed in the computer such that the result is a complex-valued Fresnel hologram. As we show, the 3D properties of the object are revealed by reconstructing this hologram in the computer.

The FINCH system is shown in Fig. 1. A white-light source illuminates a 3D object, and the reflected light from the object is captured by a CCD camera after passing through a lens L and a DOE displayed on a spatial light modulator (SLM). The specific SLM in this experiment operates in reflection mode, but it is well understood that the same principles and analysis are valid for a transmission SLM as well. In gen-

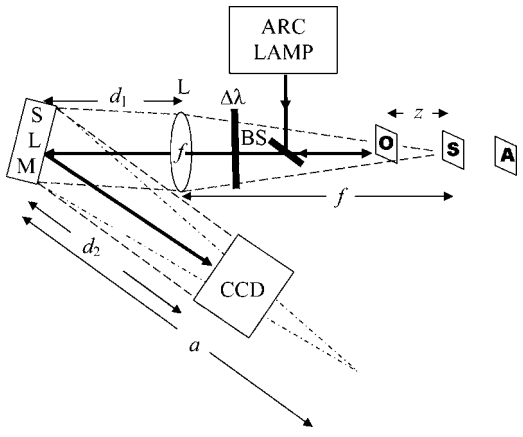

Fig. 1. Schematic of FINCH recorder. BS, beam splitter; SLM, spatial light modulator; CCD, charge-coupled device; L is a spherical lens with $f=25$ cm focal length. $\Delta\lambda$ indicates a chromatic filter with a bandwidth of $\Delta\lambda=60$ nm.

0146-9592/07/080912-3/$15.00

eral, such a system can be analyzed as an incoherent correlator, where the DOE function is considered as a part of the system's transfer function. However, in this Letter, we find it easier to regard the system as an incoherent interferometer, where the grating displayed on the SLM is considered as a beam splitter. As is common in such cases, we analyze the system by following its response to an input object of a single infinitesimal point. Knowing the system's point spread function (PSF) enables one to realize the system operation for any general object. Analysis of a beam originated from a narrowband infinitesimal point source is done using Fresnel diffraction theory,[14] since such a source is coherent by definition.

A Fresnel hologram of a point object is obtained when the two interfering beams are, for instance, plane and spherical beams. Such a goal is achieved if the DOE's reflection function $R(x_D,y_D)$ is of the form

$$R(x_D,y_D)=\frac{1}{2}+\frac{1}{2}\exp\left[-\frac{i\pi}{\lambda a}(x_D^2+y_D^2)+i\theta\right]=\frac{1}{2}+\frac{1}{2}Q\left(-\frac{1}{a}\right)\exp(i\theta), \tag{1}$$

where λ is the central wavelength, and for the sake of shortening, the quadratic phase function is designated by the function Q, such that $Q(b)=\exp[i\pi b(x^2+y^2)/\lambda]$. The constant term $\frac{1}{2}$ in Eq. (1) represents the plane wave, and the quadratic phase term is responsible for the spherical wave. The angle θ plays an important role later in the computation process to get rid of the twin image and the bias term.

A point source located at the point $(0,0,z_s)$, a distance $f-z_s$ from a spherical positive lens, with f focal length, induces a diverging spherical wave of the form of $Q[1/(f-z_s)]$ on the lens plane. Right after the lens, which has a transmission function of $Q(-1/f)$, the complex amplitude of the wave is $Q[1/(f-z_s)]\times Q(-1/f)=Q\{z_s/[f(f-z_s)]\}$. After propagating an additional distance of d_1 until the DOE plane, the complex amplitude becomes $Q\{z_s/[f(f-z_s)+z_sd_1]\}$. Right after the DOE, with the reflection function given in Eq. (1), the complex amplitude is related to $Q\{z_s/[f(f-z_s)+z_sd_1]\}[1+Q(-1/a)\exp(i\theta)]$. Finally, in the CCD plane, a distance d_2 from the DOE, the intensity of the recorded hologram is

$$I_P(x,y)=A\left|Q\left[\left(\frac{f(f-z)}{z}+d_1+d_2\right)^{-1}\right]+Q\left[\left(\frac{af(f-z)+azd_1}{za-f(f-z)-zd_1}+d_2\right)^{-1}\right]\exp(i\theta)\right|^2, \tag{2}$$

where A is a constant. The first term of Eq. (2) is now approximated to a constant by assuming that z is much smaller than f. Since the system is shift invariant, the result of $I_P(x,y)$, after calculating the square magnitude in Eq. (2), can be generalized to a PSF for any source point located at any point (x_s,y_s,z_s), as

$$I_P(x,y)=A\left(2+\exp\left\{\frac{i\pi}{\lambda\gamma(z)}\left[\left(x+\frac{ax_s}{f}\right)^2+\left(y+\frac{ay_s}{f}\right)^2\right]+i\theta\right\}+\exp\left\{\frac{-i\pi}{\lambda\gamma(z)}\left[\left(x+\frac{ax_s}{f}\right)^2+\left(y+\frac{ay_s}{f}\right)^2\right]-i\theta\right\}\right), \tag{3}$$

where $\gamma(z)=[d_2-a-z(d_1a+d_2f-af+d_2a-d_1d_2)f^{-2}]/[1-z(a+f-d_1)f^{-2}]$. For a general 3D object $g(x_s,y_s,z_s)$ illuminated by a narrowband incoherent illumination, the intensity of the recorded hologram is an integral of the entire PSFs given in Eq. (3), over all object intensity $g(x_s,y_s,z_s)$, as

$$H(x,y)\cong A\left(C+\int\int\int g(x_s,y_s,z_s)\times\exp\left\{\frac{i\pi}{\lambda\gamma(z)}\left[\left(x+\frac{ax_s}{f}\right)^2+\left(y+\frac{ay_s}{f}\right)^2\right]+i\theta\right\}dx_s dy_s dz_s+\int\int\int g(x_s,y_s,z_s)\exp\left\{\frac{-i\pi}{\lambda\gamma(z)}\left[\left(x+\frac{ax_s}{f}\right)^2+\left(y+\frac{ay_s}{f}\right)^2\right]-i\theta\right\}dx_s dy_s dz_s\right). \tag{4}$$

Besides a constant term C, Eq. (4) contains two terms of correlation between an object and a quadratic phase z-dependent function, which means that the recorded hologram is indeed a Fresnel hologram. To remain with a single correlation term out of the three terms given in Eq. (4), we follow the usual procedure of on-axis digital holography.[15] Three holograms of the same object are recorded, each with a different phase constant θ. The final hologram H_F is a superposition according to the following:

$$H_F(x,y)=H_1(x,y)[\exp(-i\theta_3)-\exp(-i\theta_2)]+H_2(x,y)[\exp(-i\theta_1)-\exp(-i\theta_3)]+H_3(x,y)[\exp(-i\theta_2)-\exp(-i\theta_1)], \tag{5}$$

where H_k is the kth recorded hologram with the phase constant θ_k. We are aware of work suggesting on-axis digital holography by a single exposure for object recognition purposes.[16] A single exposure enables one to record holograms of moving objects or to record them in a vibrating environment. However, the twin image problem presented in this single exposure technique is completely eliminated by the three exposure method performed here. A 3D image $s(x,y,z)$ can be reconstructed from $H_F(x,y)$ by calculating the Fresnel propagation formula as

$$s(x,y,z) = H_F(x,y) * \exp\left[\frac{i\pi}{\lambda z}(x^2+y^2)\right], \qquad (6)$$

where the asterisk denotes a 2D convolution.

The system shown in Fig. 1 has been used to record the three holograms. The SLM (Holoeye HEO 1080P) is phase only, and as so, the desired function given by Eq. (1) cannot be directly displayed on this SLM. To overcome this obstacle, we chose to display the phase function $Q(-1/a)$ on only half of the SLM pixels. The rest of the pixels were modulated with a constant phase, where the pixels of each kind were selected randomly. By this method, the SLM function becomes a good approximation to $R(x,y)$ of Eq. (1). Note that although the light passes a chromatic bandpass filter and therefore becomes partially temporal coherent, the illumination is still spatially incoherent. Hence, the suggested randomized pixel modulation does not introduce any speckle noise on the recorded holograms.

The SLM has 1920×1080 pixels in a display of 16.6 mm $\times$ 10.2 mm, where only the central 1024×1024 pixels were used for implementing the DOE. The phase distribution of the three reflection masks displayed on the SLM, with phase constants of 0°, 120°, and 240°, are shown in Figs. 2(a)–2(c), respectively. The other specifications of the system are: $f = 250$ mm, $a = 430$ mm, $d_1 = 132$ mm, $d_2 = 260$ mm.

Three white-on-black letters each of the size 2 mm $\times$ 2 mm were located at the vicinity of the rear focal point of the lens. O was at $z = -24$ mm, S was at $z = -48$ mm, and A was at $z = -72$ mm. These letters were illuminated by a mercury arc lamp (Zeiss-AttoArc 2, HBO 100 W). A filter that passed a Poisson-like power spectrum from 574 to 725 nm light with a peak wavelength of 599 nm and a bandwidth (full width at half maximum) of 60 nm was positioned between the beam splitter and the lens L. The three holograms, each for a different phase constant of the DOE, were recorded by using a cooled CCD camera (Hamamatsu Digital Camera C4742-95) and processed by a PC. The final hologram $H_F(x,y)$ was calculated according to Eq. (5), and its magnitude and phase distribution are depicted in Figs. 2(e) and 2(f), respectively.

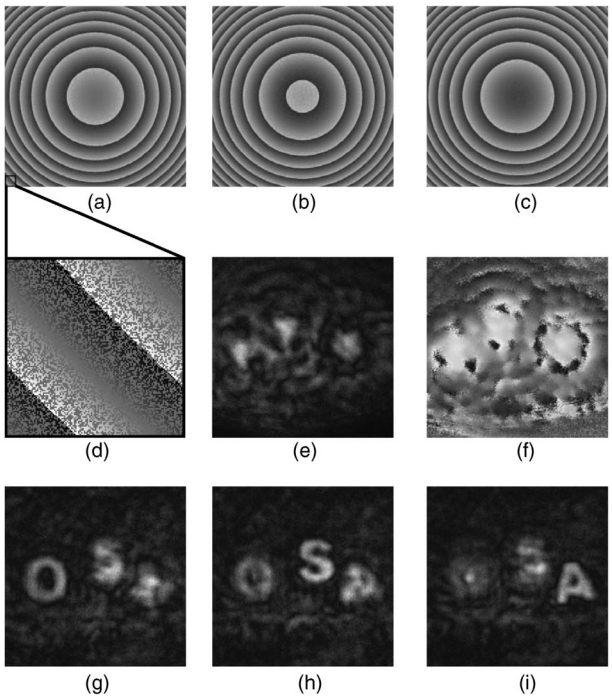

Fig. 2. (a) Phase distribution of the reflection masks displayed on the SLM, with $\theta = 0°$, (b) $\theta = 120°$, (c) $\theta = 240°$. (d) Enlarged portion of (a) indicating that half (randomly chosen) of the SLM's pixels modulate light with a constant phase. (e) Magnitude and (f) phase of the final on-axis digital hologram. (g) Reconstruction of the hologram of the three letters at the best focus distance of O. (h) Same reconstruction at the best focus distance of S, and (i) of A.

The hologram $H_F(x,y)$ was reconstructed in the computer by calculating the Fresnel propagation toward various propagation distances according to Eq. (6). Three different reconstruction planes are shown in Figs. 2(g)–2(i). In each plane, a different letter is in focus as is indeed expected from a holographic reconstruction of an object with a volume.

In conclusion, we have proposed and demonstrated a process of recording holograms of realistic 3D objects illuminated by incoherent light. Since the FINCH system has only a single channel, it does not demand complicated alignment. We anticipate that the concept of the present system can be applied to the design for a portable and very simple holographic camera, which might be useful for various applications in the fields of microscopy, still and video photography, astronomy, and medical imaging.

J. Rosen's e-mail address is rosen@ee.bgu.ac.il.
*On leave from the Department of Electrical and Computer Engineering, Ben-Gurion University of the Negev, P.O. Box 653, Beer-Sheva 84105, Israel.

References

1. J. B. Breckinridge, Appl. Opt. **13**, 2760 (1974).
2. G. Indebetouw, A. El Maghnouji, and R. Foster, J. Opt. Soc. Am. A **22**, 892 (2005).
3. A. W. Lohmann, J. Opt. Soc. Am. **55**, 1555 (1965).
4. G. W. Stroke and R. C. Restrick, Appl. Phys. Lett. **7**, 229 (1965).
5. G. Cochran, J. Opt. Soc. Am. **56**, 1513 (1966).
6. P. J. Peters, Appl. Phys. Lett. **8**, 209 (1966).
7. H. R. Worthington, Jr., J. Opt. Soc. Am. **56**, 1397 (1966).
8. A. S. Marathay, J. Opt. Soc. Am. A **4**, 1861 (1987).
9. G. Sirat and D. Psaltis, Opt. Lett. **10**, 4 (1985).
10. Y. Li, D. Abookasis, and J. Rosen, Appl. Opt. **40**, 2864 (2001).
11. Y. Sando, M. Itoh, and T. Yatagai, Opt. Lett. **28**, 2518 (2003).
12. T.-C. Poon, Adv. Imaging Electron Phys. **126**, 329 (2003).
13. L. Mertz and N. O. Young, in *Proceedings of Conference on Optical Instruments and Techniques*, K. J. Habell, ed. (Chapman & Hall, 1961), p. 305.
14. J. Goodman, *Introduction to Fourier Optics*, 2nd ed. (McGraw-Hill, 1996), Chap. 4, pp. 63–95.
15. I. Yamaguchi and T. Zhang, Opt. Lett. **22**, 1268 (1997).
16. D. Kim and B. Javidi, Opt. Express **12**, 5539 (2004).